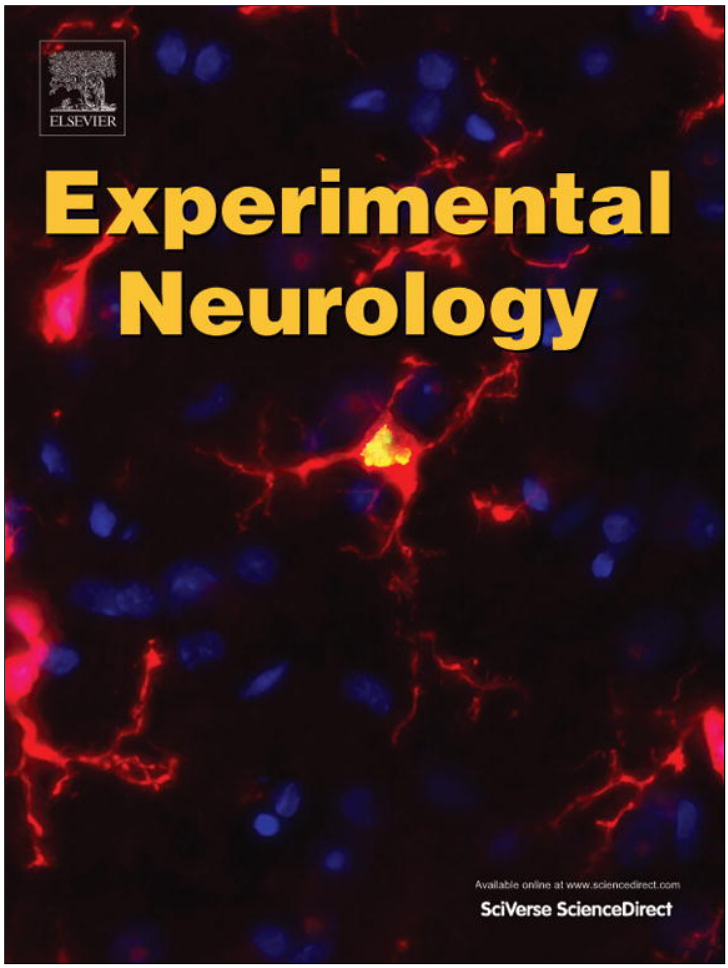

Experimental Neurology 248 (2013) 236–245

Contents lists available at SciVerse ScienceDirect

Experimental Neurology

journal homepage: www.elsevier.com/locate/yexnr

Increased excitability in serotonin neurons in the dorsal raphe nucleus in the 6-OHDA mouse model of Parkinson's disease

Alexander Prinz [a,1], Lisa-Marie Selesnew [a,1], Birgit Liss [b], Jochen Roeper [a], Thomas Carlsson [a,b,*]

[a] Institute of Neurophysiology, Neuroscience Center, Goethe University Frankfurt, Theodor Stern Kai 7, 60590 Frankfurt am Main, Germany
[b] Institute of Applied Physiology, University of Ulm, Albert-Einsteinallee 11, 89081 Ulm, Germany

ARTICLE INFO

Article history:
Received 18 February 2013
Revised 23 May 2013
Accepted 16 June 2013
Available online 26 June 2013

Keywords:
5-HT
6-Hydroxydopamine
Electrophysiology
Patch-clamp
PD
In vitro

ABSTRACT

The serotonin system has recently been demonstrated to have an important role in Parkinson's disease, in particular in response to L-DOPA treatment. It has been shown that central serotonin neurons convert peripherally administered L-DOPA to dopamine. Striatal dopamine release by these serotonin neurons is believed to be a main player in the induction of the troublesome L-DOPA-induced dyskinesias, which develops in patients within 5–10 years after the use of the drug. Electrophysiological characterization of midbrain dopamine neurons and dorsal raphe nucleus serotonin neurons has further revealed close interaction between these two cells groups. These data indicate that the loss of dopamine neurons and fibers alone and following L-DOPA treatment might change the electrophysiological properties of the serotonin neurons in the dorsal raphe nucleus. Although in vivo data have indicated changes in firing properties following dopamine depletion by 6-OHDA, the data have been conflicting. We therefore investigated the electrophysiological properties of serotonin neurons following dopamine degeneration and L-DOPA treatment in the 6-OHDA-lesion mouse model of Parkinson's disease using in vitro patch clamp technique in acute slices. We found that 6-OHDA lesions alone significantly increased spontaneous and maximal firing discharges of serotonin neurons, which were accompanied by respective changes in the action potential waveforms. L-DOPA treatment did not reverse this increase in spontaneous frequency, but partially normalized AP properties. Our data demonstrate that the intrinsic excitability of serotonin neurons is altered in response to both dopamine degeneration as well as subsequent L-DOPA treatment. This lesion- and treatment-induced plasticity of the serotonin might contribute to its role in L-DOPA induced dyskinesia.

Introduction

Parkinson's disease (PD) is characterized by the progressive loss of dopamine (DA) in the nigrostriatal pathway, resulting in motor symptoms including bradykinesia/akinesia (slowness/absence of movements), tremor and postural imbalance. The gold standard disease therapy is based on restoring the DA concentration in the brain using the DA precursor L-DOPA (in combination with peripheral amino-acid decarboxylase [AADC] inhibitors), which is converted in the brain to DA. It has recently been demonstrated that the serotonin system plays a major role in the conversion of peripherally administered L-DOPA to DA at multiple sites in the brain, including the striatum and substantia nigra (SN), after complete DA depletion (Navailles et al., 2010a). In fact, serotonin neurons do not only convert exogenous delivered L-DOPA to DA, but also store it and release it in an activity-dependent manner (Arai et al., 1994, 1995, 1996; Hollister et al., 1979; Ng et al., 1970, 1971). This suggests that the "DA production" in the serotonin neurons may be responsible for both functional effects of L-DOPA treatment, as well as side effects caused by the same medication in more severe stages of PD, when the majority of the DA neurons and fibers are lost in the brain. In fact, the development of L-DOPA-induced dyskinesias has been tightly associated with DA release from serotonin neurons in both rodent and non-human primates (Bezard et al., 2013; Carlsson et al., 2007; Carta et al., 2007; Munoz et al., 2008; Rylander et al., 2010), as well as indication in human PD (Bonifati et al., 1994; PsychoGenic, Eltoprazine, press release June 12, 2012).

Interestingly, the midbrain [including the SN and ventral tegmental area (VTA)] receives the densest serotonin innervation in the brain of humans and several animal species including rodents (Mackay et al., 1978; Moukhles et al., 1997). Serotonin fiber projections, originating in the dorsal raphe nucleus (DRN), also innervate DA axonal target areas such as the caudate putamen (Di Giovanni et al., 2008). In addition, a proportion of DA fibers from the SN and VTA also projects

* Corresponding author at: Sahlgrenska Academy, Institute of Neuroscience & Physiology, Section for Pharmacology, Medicinaregatan 13, 405 30 Gothenburg, Sweden. Fax: +49 69 63016987.
E-mail addresses: carlsson@em.uni-frankfurt.de, thomas.carlsson.2@gu.se (T. Carlsson).
[1] Equal contributing author.

0014-4886/$ – see front matter © 2013 Elsevier Inc. All rights reserved.
http://dx.doi.org/10.1016/j.expneurol.2013.06.015

back to the raphe nucleus, as demonstrated by both retrograde tracing and the expression of DA D_2-receptor on the DRN serotonin neurons (Haj-Dahmane, 2001; Kitahama et al., 2000). It has been extensively reported that DA and serotonin systems have multiple connections, most importantly functional electrophysiological interactions (for review see Di Giovanni et al., 2008). About a handful of studies have investigated the in vivo electrophysiological effect on DRN serotonin neurons in response to DA neurodegeneration induced by 6-OHDA in the rat PD model, however the data have shown inconsistent results, where increased, decreased or unchanged firing properties in DRN serotonin neurons were evident after DA depletion (Chu et al., 2004; Guiard et al., 2008; Wang et al., 2009; Zhang et al., 2007). However, effects of 6-OHDA lesions on in vitro electrophysiology of DRN serotonin neurons in acute slices, as well as those of sequential DA replacement therapy, i.e. L-DOPA treatment, are unknown. Therefore, in order to further clarify the effect of DA lesions, we investigated the electrophysiological properties of identified serotonin neurons in the DRN in normal mice, after unilateral intrastriatal 6-OHDA lesion, and subsequent L-DOPA-treatment using in vitro patch clamp technique. We confirm that 6-OHDA, 3–4 weeks post lesion, significantly increases both spontaneous and maximal firing discharges. These changes, in addition, were associated with alterations of action potential (AP) waveforms. Following L-DOPA therapy in 6-OHDA lesioned animals, the spontaneous discharge was not significantly changed, but AP properties such as duration were normalized after the DA replacement therapy.

Material and methods

Animals

In this study 57 adult (12–20 weeks old) male C57/B6 mice (Charles-River, GmbH, Germany), weighing >25 g in the beginning of the experiment, were used. The animals were housed with free access of water and food with standard 12 h/12 h light/dark cycle. All surgeries and preparations were performed according to ethical guidelines approved by the Regierungspräsidium Darmstadt, Germany (V54-19c 20/15-F 40/31).

6-OHDA lesion/sham-operation

The lesion and sham-operation surgery was performed under 1–2% isoflurane (in 100% O_2, Forene, Abbott, Wiesbaden, Germany) anesthesia. In order to achieve a partial unilateral lesion of the nigrostriatal pathway, or sham-operation, the animals received two injections, each of 2 μl, of 6-OHDA (D4381, Sigma-Aldrich, Steinheim, Germany; 3.2 μg/μl in 0.2% L-ascorbic acid-saline) or of 0.2% L-ascorbic acid-saline, into the striatum, while placed in a stereotactic frame (Kopf instruments, Tujunga, CA) fitted with a 10 μl syringe and 33-Gauge blunt needle (WPI Inc., Sarasota, FL). The anteroposterior (AP), mediolateral (ML), and dorsoventral (DV) coordinates for the two injections were: I): AP: +1.0 mm, ML: −2.1 mm, DV: −2.9 mm; and II) AP: +0.3 mm, ML: −2.3 mm and DV: −2.9 mm, in relation to bregma and dura in a flat skull position. The 6-OHDA or ascorbic acid-saline was injected at a rate of 0.5 μl/min using a minipump (Micro4, WPI Inc.), and the needle was kept in place for at least 3 min before it was slowly retracted, to avoid backflow. Before surgery Desipramine (25 mg/kg; D3900, Sigma-Aldrich) was injected 30 min prior to the 6-OHDA injections, to protect unselective damage to the noradrenergic system. Further, atropine was injected 15 min before surgery to prevent heart failures during operation. Paracetamol (4% Ben-u-ron saft, Bene Arzneimittel, Munich, Germany) was used in the drinking water, or subcutaneous injections of Carpofen (5 mg/kg) were used as post-operative pain treatment for the first 24 h post surgery.

L-DOPA treatment

Twelve animals [normal controls (n = 2) and sham-operated controls (n = 3); and 6-OHDA-lesions (n = 7)] received daily subcutaneous injections of 6 mg/kg L-DOPA methyl-ester (D1507, Sigma-Aldrich), in combination with the aminoacid decarboxylase inhibiter Benserazide (10 mg/kg; D7283, Sigma-Aldrich). The 6-OHDA and sham-operated animals received their first injections at two weeks post surgery for 10–14 days. The L-DOPA dose, timing of the initiation and duration of the drug and the patch-clamp recording were based on first: 6 mg/kg is shown to be the lowest dose of L-DOPA that can improve the functional behavior in severe 6-OHDA lesioned rodents (comparable to therapeutic doses in PD patients; Kirik et al., 2002); second: it was important that the time following 6-OHDA lesion was the same [at 21–28 days — at which time the majority of the DA neurons in the SN has degenerated (Alvarez-Fisher et al., 2008)] for the drug-naïve/vehicle and L-DOPA-treated animals in the 6-OHDA groups; third: the L-DOPA was introduced later than one week after the 6-OHDA injection, as the major loss of DA cells in the SN is within the first 7 days (Alvarez-Fisher et al., 2008); and fourth the sub-chronic L-DOPA treatment of 10–14 days using the selected dose develops signs of dyskinesias in severely DA lesioned rodents (Lundblad et al., 2004).

Electrophysiology

Slice preparation

At 21–28 days post 6-OHDA lesion (36–48 h post last L-DOPA-injection) or sham-lesion, 225 μm thick coronal slices of the brain stem including the DRN were prepared as previously described (Lammel et al., 2008). Briefly, mice were anesthetized by an overdose of Ketamine (500 mg/10 ml; Ratiopharm, Ulm, Germany) and Dormitor (1 mg/ml, Pfizer GmbH, Berlin, Germany). Heparin (100 μl; 25,000 I.E./5 ml, Ratiopharm) was infused intracardially, followed by transcardial perfusion with ice-cold artificial cerebrospinal fluid (ACSF) solution containing in mM/l: 125 NaCl, 2.5 KCl, 25 $NaHCO_3$; 1.25 NaH_2PO_4, 2.5 Glucose, 50 Sucrose, 6.174 $MgCl_2$, 0.1 $CaCl_2$ and 2.96 Kynurenic Acid (Sigma-Aldrich), bubbled with carbogen gas (95% O_2 and 5% CO_2), for 5–7 min at a flow rate of about 10–15 ml/min. The brains were rapidly removed and the DRN were sliced at 225 μm thick coronal sections using a Vibratome (VT1200S, Leica Microsystems, Wetzlar, Germany). The slices were directly transferred to carbogen bubbled ACSF (in mM/l: 125 NaCl, 2.5 KCl, 25 $NaHCO_3$; 1.25 NaH_2PO_4, 2.5 Glucose, 22.5 Sucrose, 2.058 $MgCl_2$, and 2 $CaCl_2$), and allowed to recover for at least 1.5 h at 37 °C before in vitro patch clamp measurements.

Whole cell patch-clamp recording

In order to perform patch clamp recordings the slices containing the DRN were transferred to a heated (37 °C) chamber, continuously perfused with 2–4 ml/min carbogen bubbled ACSF, including 4 μM non-NMDA glutamate receptor antagonist (CNQX; Biotrend AG, Zurich, Switzerland) and 10 μM $GABA_A$ receptor antagonist (SR95531; Biotrend AG, Zurich, Switzerland). Slices from three animals were also perfused without the $GABA_A$ blocker, in order evaluate the frequency of spontaneous firing neurons without this inhibition. Borosilicate glass pipettes (GC150TF-10, Harvard Apparatus, Kent, UK) were pulled (DMZ Universal puller, Zeitz Instruments GmbH, Munich, Germany) with 2.9–4.7 MΩ tip resistance (average: 3.6 ± 0.027). The pipettes were filled with internal solution containing [in mM/l: 135 K-gluconate, 5 KCl, 10 HEPES, 0.1 EGTA, 2 $MgCl_2$, 0.2 Li_2GTP, 2 Na_2ATP and 1 μg/μl Neurobiotin (NB); pH = 7.35 with KOH (270–300 mOsm)]. The DRN and the serotonin cells were visualized by infrared differential contrast videomicroscope fitted with digital camera (VX55, Photonics, Pittsfield, MA), mounted to an upright microscope (Axioskop 2, FSplus, Zeiss, Jena, Germany). Recordings in current clamp were collected using the EPC-10 amplifier (HEKA electronics, Lambrecht, Germany) and Patch

Master v.2.43 software (HEKA electronics). Cells that displayed continuous spontaneous pacemaker activity over 5 sweeps, each 5 s, with an uncompensated series resistance of <20 MΩ were collected for analysis.

Data analysis

The patch-clamp whole-cell recordings were digitized at 20–50 kHz. Spontaneous and evoked firing frequencies, subthreshold and action potential waveforms were analyzed using Fit master (HEKA electronics) and IGOR pro v6.02a fitted with Neuromatic v2.00 (WaveMetrics Inc., Lake Oswego, OR).

Histological analysis

The forebrains of the animals used for in vitro patching were fixed in 4% PFA (in 0.1 M phosphate buffer) for 24–48 h, and transferred into a storing solution containing 10% sucrose, 0.05% NaN_3 in PBS. All forebrains were further sliced at 35 μm slices through the striatum using a freezing slide-microtome (VT1000S, Leica Microsystems) before immunohistochemically visualized for tyrosine hydroxylase (TH), serotonin, and serotonin transporter (SERT) proteins. The patched sections (225 μm) were following electrophysiological measurements fixed in 2% PFA (in 0.1 M phosphate buffer, pH 7.4) for 1–3 h, thereafter they were stored in a storing solution for at least 24 h until processes for serotonin, TH and NB stainings.

Immunohistochemistry

The free-floating sections were first rinsed in PBS, before non-specific binding were blocked by a 1 h pre-incubation in 5% appropriate normal serum containing 0.25% Triton X-100 for the striatal (35 μm) section, and 5% normal serum containing 2% Triton X-100, for the 225 μm patch sections dissolved in PBS. This step was followed by incubation (overnight for the striatal 35 μm sections and over two nights for the patched 225 μm sections) in room temperature with appropriate primary antibodies in the same respective solution as for the blocking step. Here we used the rabbit anti-TH (1:1000; #657012; Calbiochem, EMD Chemicals, San Diego, CA) and the rabbit anti-SERT (1:1000; Immunostar, Hudson, WI), as primary antibodies, to separately stain the fiber network in the striatum (in the 35 μm sections) to assess the lesion size in the two systems. For the identification of the patched neurons (in the 225 μm sections) we used the mouse anti-TH (1:1000; MAB318; Millipore, Temacula, CA) co-stained with rabbit anti-serotonin (5-HT; 1:1000; Immunostar, Hudson, WI). For the representation of the coronal levels of the DRN in Fig. 2F, we used a concentration of 1:4000 (instead of 1:1000) of the 5-HT antibody, due to the smaller section thickness. On the 2nd or 3rd day respectively the sections were rinsed 3 times with PBS, followed by incubation in appropriate secondary fluorescence antibodies (1:1000 goat anti-rabbit Alexa 488 for serotonin; 1:1000 goat anti-mouse Alexa 647 for TH; and streptavidin 568 for NB; all Invitrogen, Darmstadt, Germany) or biotinylated secondary antibody [1:1000 goat anti-rabbit for TH and SERT; Vector Laboratories, Burlingame, CA]. The incubation time for the secondary antibodies were 1 h for the 35 μm sections for 3,3′-diaminobenzidine (DAB), and overnight for the in vitro patched 225 μm sections. For the fluorescence stainings the sections were rinsed additional 3 times in PBS before being mounted on glass slides and coverslipped with Vectashield™ (H-1400; Vector Laboratories). The sections taken for the DAB staining were, following the secondary antibody incubation, rinsed 3 times in PBS, incubated 1 h with Avidin-Biotin complex (ABC Elite standard, PK-6100, Vector Laboratories) before visualization with DAB (SK-4100, Vector Laboratories) and H_2O_2. The sections were mounted on gelatinized glass slides, dehydrated in ascending alcohol solutions and cleared in Xylene, and finally coverslipped with DEPEX mounting medium (VWR International Ltd, Poole, UK).

Morphological analysis

Confocal microscopy

In order to confirm the nature of the cells patched, Laser scanning microscope was used (EZ C1, Nikon GmbH, Düsseldorf, Germany). Florocromes Alexa 488, 568 and 647 were excited by Argon laser using appropriate filters, where serotonin was excited in green, NB in red and TH in far-red (visualized in blue on Fig. 2E).

Estimation of TH- and SERT-positive fiber innervations in the striatum

The DA and serotonin fiber densities in the striatum were evaluated from TH- and SERT-positive staining. Briefly, images were taken through 7 rostral-caudal levels (AP: +1.2 mm, +0.9 mm, +0.6 mm, +0.3 mm, 0.0 mm, −0.3 and −0.9 mm, relative from bregma) using an Olympus BX61 microscope with 2×/0.05 objective. Cortex, where no DA fibers where evident, was used as background level for the TH density and corpus callosum was used as background for the SERT density. The whole striatum was outlined as previously described (Carlsson et al., 2007), and the optional density was evaluated by ImageJ v 1.44o (for MacOsX platform; NIH, http://rsb.info.nih.gov/ij/). The data are expressed as optical density in percentage of the control side.

Statistical analysis

All statistical analyses were performed with Student's unpaired *t*-test using Graphpad Prism v5.0c (Graphpad software Inc., La Jolla). The level of significance was set at $p < 0.05$. Data are presented as mean ± S.E.M.

Results

Effect of intrastriatal 6-OHDA lesions on DA and serotonin fibers in the striatum

TH- and SERT-positive fiber densities were evaluated throughout the striatum at seven coronal sections, as described above. At 21–28 days after 6-OHDA injections, TH-immunoreactivity indicated a robust and significant DA lesion within the striatal complex to 28.1 ± 5.5% of intact side (n = 8; Figs. 1A–C), as compared to control animals (103.1 ± 3.2% of intact side; n = 5; Student's unpaired *t*-test, $p < 0.0001$). L-DOPA injections did not alter the extent of the 6-OHDA lesions (37.4 ± 3.1% of intact side, n = 7). In contrast, the SERT-immunoreactivity showed no lesion or hyperinnervation of serotonin fibers in the striatum (110.5 ± 1.9% of intact side, n = 7), after 6-OHDA lesion, as compared to controls, 110.0 ± 1.5% of intact side (n = 5; Figs. 1D–F). Also, L-DOPA treatment did not affect the SERT immunoreactivity in the striatum of 6-OHDA-treated animals (108.9 ± 1.4% of intact side).

Electrophysiological properties of adult identified serotonin neurons in the DRN

Electrophysiological properties including spontaneous firing (Fig. 2A), the action potential (AP) waveform properties (Fig. 2B), subthreshold properties such as sag amplitudes and rebound delays (Fig. 2C), as well as current-evoked maximal firing frequencies (Fig. 2D) were characterized in control (n = 14) and sham-operated (n = 3) animals. Out of a total of 104 whole-cell recorded and spontaneously firing neurons in the DRN, 87 were successfully labeled with NB and immunohistochemically identified as serotonin neurons (84%; Fig. 2E). These identified serotonin neurons were distributed across the full rostro-caudal range of the DRN with the majority localized close to midline, and lesser neurons in the lateral wings of the DRN (Figs. 2F, G). In the presence of the selective $GABA_A$ receptor blocker SR95531 (10 μM), 80–90% of the patched serotonin DRN neurons fired spontaneously in high quality coronal brain slices from adult mouse, which were achieved by combined intravascular perfusion with ice-cold neuroprotective solutions followed by careful slicing using

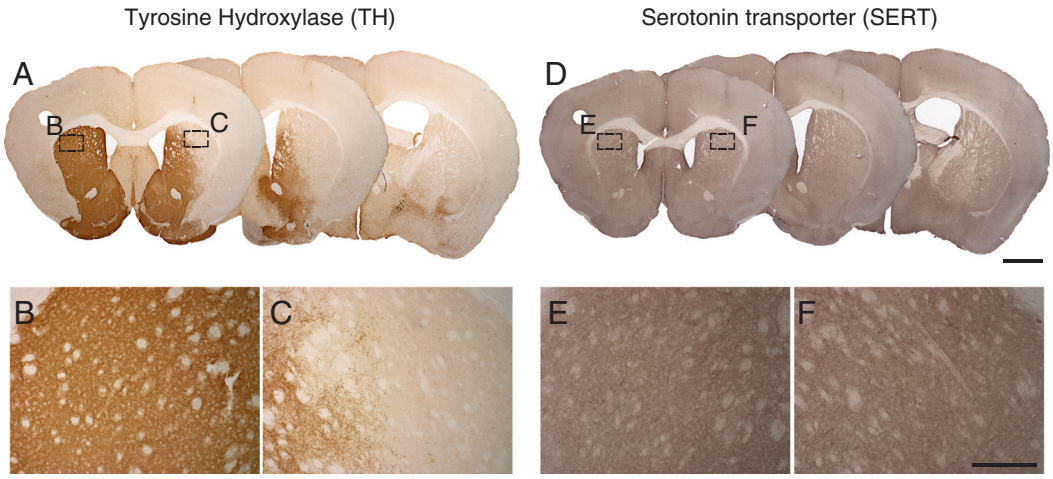

Fig. 1. TH- and SERT-positive fiber innervation in the striatum following 6-OHDA lesion. TH-positive staining revealed a severe loss of DA fibers in the striatum (A; compare intact B and lesion side C). The lateral and dorsal striatum is almost completely denervated throughout the rostrocaudal axis, while the nucleus accumbens and the rostromedial striatum, which is mainly projected from the VTA, are relatively spared in this intrastriatal lesion. The SERT-positive staining revealed that no lesion or hyperinnervation of the serotonin fibers was present in the striatum following the 6-OHDA-induced DA lesion (D; compare intact E and lesion side F). Scale bar in D (apply to A and D) and F (apply to B, C, E and F) represent 1 mm and 200 μm respectively.

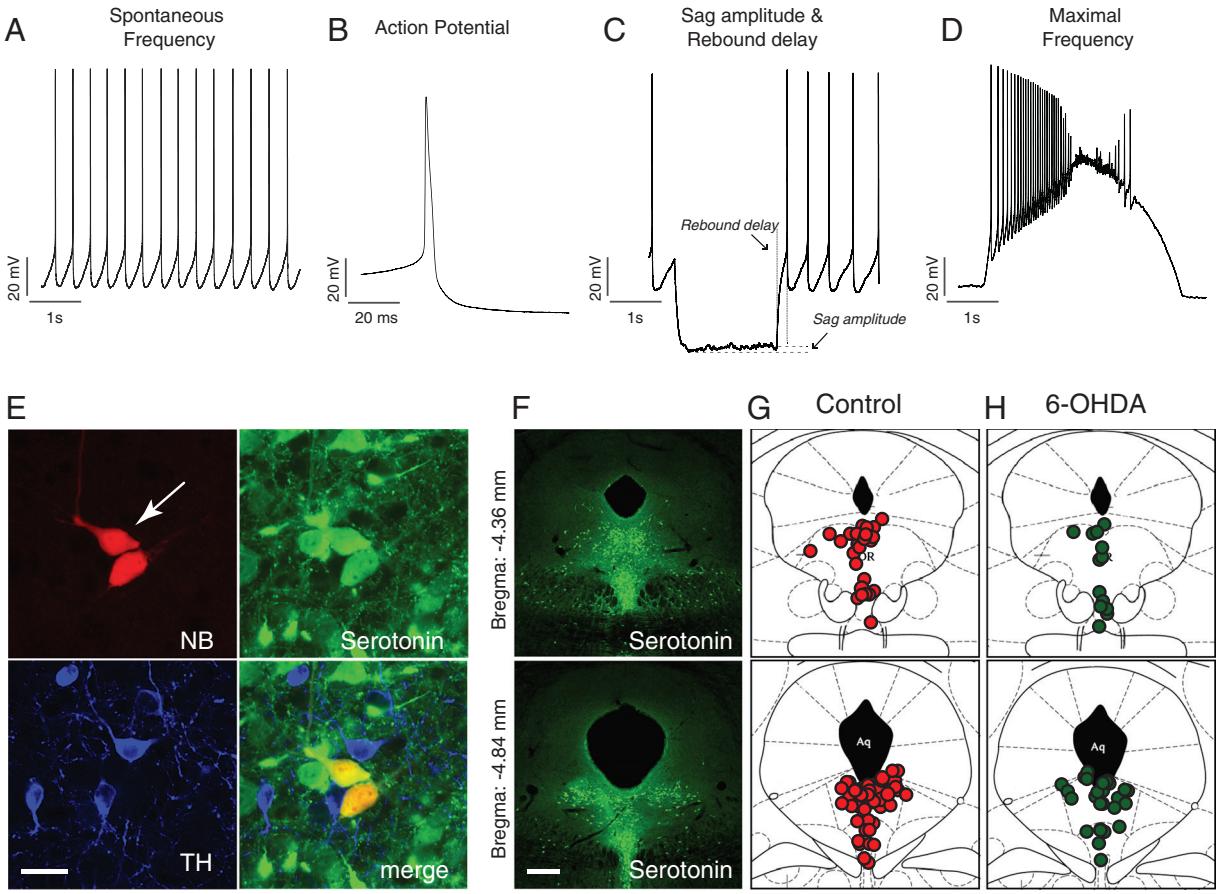

Fig. 2. Basic electrophysiological properties and recorded serotonin neurons in the DRN. Electrophysiological properties such as spontaneous pacemaker frequency (A), the action potential (AP) and its properties (B), Sag amplitude and rebound delay using a hyperpolarization protocol, and Maximal firing using depolarization protocol (D), were investigated in this study. The recorded DRN serotonin cells were visualized by neurobiotin (NB; Red — steptavidin 568) labeling, and the sections were fluorescence co-immunostained using serotonin antibody (green — Alexa 488), and tyrosine hydroxylase (TH) antibody (Blue — Alexa 647) (E). The patched and recorded serotonin neurons were distributed over the whole rostrocaudal axis of the DRN in both controls (G) and 6-OHDA lesion animals (H). The cells were located mainly in the midline and less in the lateral wings. Serotonin staining of the two mapped levels is represented in panel F. The electrophysiological properties in panel A–D represent the top cell visualized in E (white arrow) with an average spontaneous firing of 2.3 Hz (first sweep 2.8 Hz), maximal firing of 26.4 Hz, Sag amplitude & rebound delay of 3.1 mV and 147.9 ms, respectively, and AP duration of 4.5 ms. The second cell in panel E was also individually recorded (data not shown). Scale bar in A and B represents 20 μm and 250 μm, respectively. (For interpretation of the references to color in this figure legend, the reader is referred to the web version of this article.)

the Leica VT1200S vibratome (see methods for details). For comparison, in the absence of $GABA_A$ receptor inhibition, only about half of the serotonin DRN neurons patched were spontaneously active (n = 8 of 17 cells; 47%). The remaining electrically silent neurons showed slightly hyperpolarized membrane potentials (−53.4 ± 4.8 mV, n = 8) and started to fire action potentials upon injection of small depolarizing currents (11.3 ± 5.3 pA; n = 8 from three animals). This physiological state is consistent with the presence of tonic local inhibition via GABA interneurons in the DRN (Jolas and Aghajanian, 1997). Thus, we were able to study a functionally homogeneous serotonin DRN neuronal population in the presence of SR95531. The mean spontaneous pacemaker frequency of the identified adult serotonin DRN neurons recorded in synaptic isolation (isolated from non-NMDA glutamate and $GABA_A$, but not 5-HT_{1A} autoreceptor) was 2.2 ± 0.1 Hz (Figs. 3A, C; normal: 2.2 ± 0.1 Hz, n = 66 versus sham-operated: 2.0 ± 0.4 Hz, n = 21 showed no difference and were pooled). The spontaneous frequency showed a slowing down over the five measured sweeps, and reached at the last sweep an overall average of 74% of the initial sweep (from 2.6 ± 0.1 to 1.9 ± 0.1 Hz). The pacemaker of serotonin DRN neurons was also regular as indicated by a small coefficient of variation (CV), an arithmetic measure of regularity of spontaneous pacemaker activity (15.7 ± 0.9%, n = 87). To study the full dynamic range of firing frequencies, we applied currents ramps of increasing amplitudes to serotonin DRN neurons, which revealed a mean maximal discharge frequency of 30.4 ± 1.5 Hz before onset of depolarization block (n = 81, Figs. 3D, F).

Analysis of the AP waveforms (Fig. 2B) showed a mean maximum and minimum of 51.3 ± 0.4 mV and −61.0 ± 0.5 mV, respectively, and a pronounced and slow afterhyperpolarization (AHP) with a mean amplitude of 32.5 ± 0.4 mV, calculated from the AP threshold

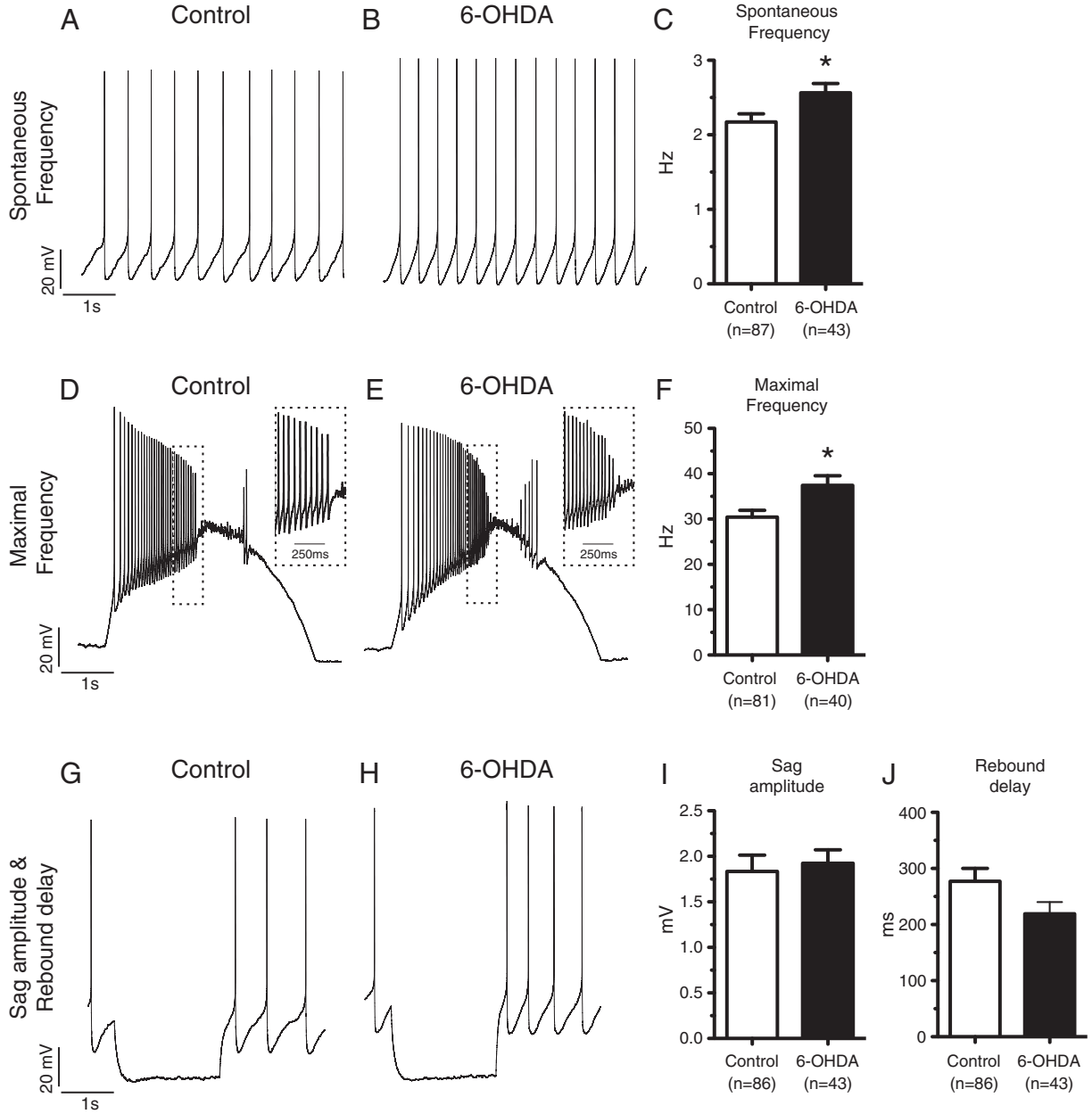

Fig. 3. Firing discharge and sag amplitude & rebound delay in normal and 6-OHDA lesioned animals. Normal animals displayed a regular pacemaker activity of 2.2 ± 0.1 Hz (A). This discharge was significantly increased after intrastriatal 6-OHDA lesion to 2.6 ± 0.1 Hz (p = 0.01; B, C). The maximal firing was also increased in the DA depleted animals (p = 0.008; E, F) as compared to neurons from normal animals/sham-operated animals (D). The sag amplitude and rebound delay were however not altered between the control (G) and the 6-OHDA lesioned animals (H, I, J) * = different from Control.

(designated at the point of upstroke velocity = 5 mV/ms; −28.5 ± 0.3 mV). The mean duration of APs at threshold was 3.5 ± 0.1 ms (n = 86, Figs. 5A, C). Using a stepwise hyperpolarizing protocol (−25 pA/sweep), all but two neurons show either no or only very small sag amplitudes (1.8 ± 0.2 mV, n = 86) when hyperpolarized to −80 mV (Figs. 2C, 3G, I). The mean post-hyperpolarization rebound delay before the first AP was 277.0 ± 23.2 ms (n = 86, Figs. 2C, 3G, J). The basic electrophysiological properties of adult identified serotonin DRN neurons are summarized in Table 1.

6-OHDA-induced electrophysiological changes in DRN serotonin neurons

At 21–28 days after the intrastriatal 6-OHDA injections, serotonin neurons (n = 45 cells from 9 animals, distributed across the rostro-caudal axis of the DRN) were recorded (Figs. 2F, H). The 6-OHDA-induced DA lesion was associated with a significant increase (+18%) in pacemaker firing to 2.6 ± 0.1 Hz (n = 45, Figs. 3B, C; Student's unpaired *t*-test, p = 0.01). Similar to the normal cells, the serotonin cells in the 6-OHDA lesioned rats showed a slowing down in spontaneous firing to 70% of the initial sweep. The post-6-OHDA recorded serotonin neurons showed also a small but significant decrease in the regularity of firing (CV of 19.2 ± 1.6%, n = 45, Student's unpaired *t*-test, p = 0.047). The increased spontaneous discharge was accompanied with a 23% increased maximum firing to 37.5 ± 2.1 Hz compared to control cells (n = 40, Figs. 3D–F; unpaired *t*-test, p = 0.008). In contrast to these firing properties, sag amplitudes and rebound delays were not significantly altered (Figs. 3G–J). Moreover, closer analysis of the AP waveforms, revealed a significantly decreased AP duration to 3.1 ± 0.1 ms (−13%; n = 45, Student's unpaired *t*-test, p = 0.002; Figs. 5B, C). Following the 6-OHDA lesion, we also note small (<10%) but significant changes in several AP waveform properties (see Table 1). In addition, the whole-cell capacitance was significantly smaller after the 6-OHDA lesion (28.9 ± 1.0 pF) as compared to cells from control animals (32.2 ± 1.0 pF; Student's unpaired *t*-test, p = 0.04), which might indicate a small reduction of size in post-6-OHDA lesion serotonin DRN neurons.

Effect of L-DOPA treatment on electrophysiological properties of serotonin DRN neurons from 6-OHDA-treated and control animals

Compared to neurons from L-DOPA-naïve 6-OHDA lesioned animals, the accelerated mean spontaneous firing frequency of serotonin DRN neurons were unaffected (2.5 ± 0.1 Hz; n = 39 cells from 7 animals) following sub-chronic L-DOPA therapy in 6-OHDA treated animals (6 mg/kg/day; 12.7 ± 0.6 days), (Figs. 4B, C). In contrast, the AP duration was significantly prolonged following L-DOPA treatment (+12% to 3.4 ± 0.1 ms; n = 38), compared to drug-naive DA lesioned animals (Student's unpaired *t*-test, p = 0.02; Figs. 5E, F). Indeed, the AP duration after L-DOPA treatment was very similar to those observed in control animals (Fig. 5A). Moreover, the CV for the spontaneous firing was not different following L-DOPA treatment in the 6-OHDA-induced DA depleted animals, 18.6 ± 2.1%. Also, the maximum firing discharge was reduced after L-DOPA treatment (33.8 ± 2.0 Hz, n = 36), and no longer significantly different from controls (Figs. 4E, F). Finally, the mean input resistance was higher in serotonin DRN neurons from 6-OHDA lesioned animals, which were treated with L-DOPA in contrast to those from lesioned L-DOPA-naïve animals (+14%; 666.8 ± 41.3 MΩ (n = 45) vs. 582.5 ± 26.7 MΩ (n = 39); Student's unpaired *t*-test, p = 0.044; Table 1).

In non-lesioned animals treated with L-DOPA (6 mg/kg/day, 11.6 ± 0.8 days), the spontaneous firing discharge was also increased compared to drug-naïve non-lesioned controls (+27%; 2.8 ± 0.3 Hz, n = 30; Student's unpaired *t*-test, p = 0.009; Figs. 4A, C), and a trend was observed for higher maximal firing frequencies (36.0 ± 2.5 Hz, n = 27; Student's unpaired *t*-test, p = 0.06; Figs. 4D, F).

Table 1
Electrophysiological properties in normal, 6-OHDA-lesioned, and L-DOPA-treated animals.

					Action potential								
	Frequency (Hz)	Maximal firing (Hz)	Sag amplitude (mV)	Rebound delay (ms)	Amplitude (mV)	Maximum (mV)	Minimum (mV)	Duration (ms)	Threshold (ms)	AHP (mV)	Minimum time to depol. peak (ms)	Input Resistance (MQ)	Capacitance (pF)
Control (n = 81–87)	2.2 ± 0.1	30.4 ± 1.5	1.8 ± 0.2	277.0 ± 23.2	79.8 ± 0.6	51.3 ± 0.4	−61.0 ± 0.5	3.5 ± 0.1	−28.5 ± 0.3	32.5 ± 0.4	45.7 ± 2.3	588.7 ± 19.2	32.2 ± 1.0
6-OHDA (n = 40–46)	2.6 ± 0.1*	37.5 ± 0.2*	1.9 ± 0.1	204.9 ± 22.0	82.7 ± 0.9*	53.5 ± 0.7*	−59.9 ± 0.7	3.1 ± 0.1*	−29.2 ± 0.4	−30.6 ± 0.5*	42.0 ± 2.5	582.5 ± 26.7	28.9 ± 1.0*
Control L-DOPA (n = 27–30)	2.8 ± 0.3*	36.0 ± 2.5	1.5 ± 0.3	219.2 ± 21.0	78.5 ± 1.1	50.1 ± 0.9	−61.1 ± 1.0	3.2 ± 0.1	−29.4 ± 0.5	−32.7 ± 0.9	49.0 ± 3.3	621.4 ± 32.5	31.9 ± 2.0
6-OHDA L-DOPA (n = 36–39)	2.5 ± 0.1	33.8 ± 2.0*	1.3 ± 0.2*	220.0 ± 17.5	81.1 ± 0.9	51.9 ± 0.7	−62.3 ± 0.8*	3.4 ± 0.1*	−29.2 ± 0.4	−33.1 ± 0.7*	50.1 ± 2.6*	666.8 ± 31.9*	29.3 ± 1.3

Note: Following 6-OHDA lesion spontaneous frequency and maximal frequency (F_{MAX}) were significant higher as compared to control animals. This was accompanied with minor, but significant, changes in the properties of the action potential. Interestingly, the capacitance was decreased in the 6-OHDA lesioned animals, which may indicate a smaller and degenerated cell after 6-OHDA lesion. * = significant from Control group; # significant from respective untreated group; Student's unpaired t-tests, $p < 0.05$.

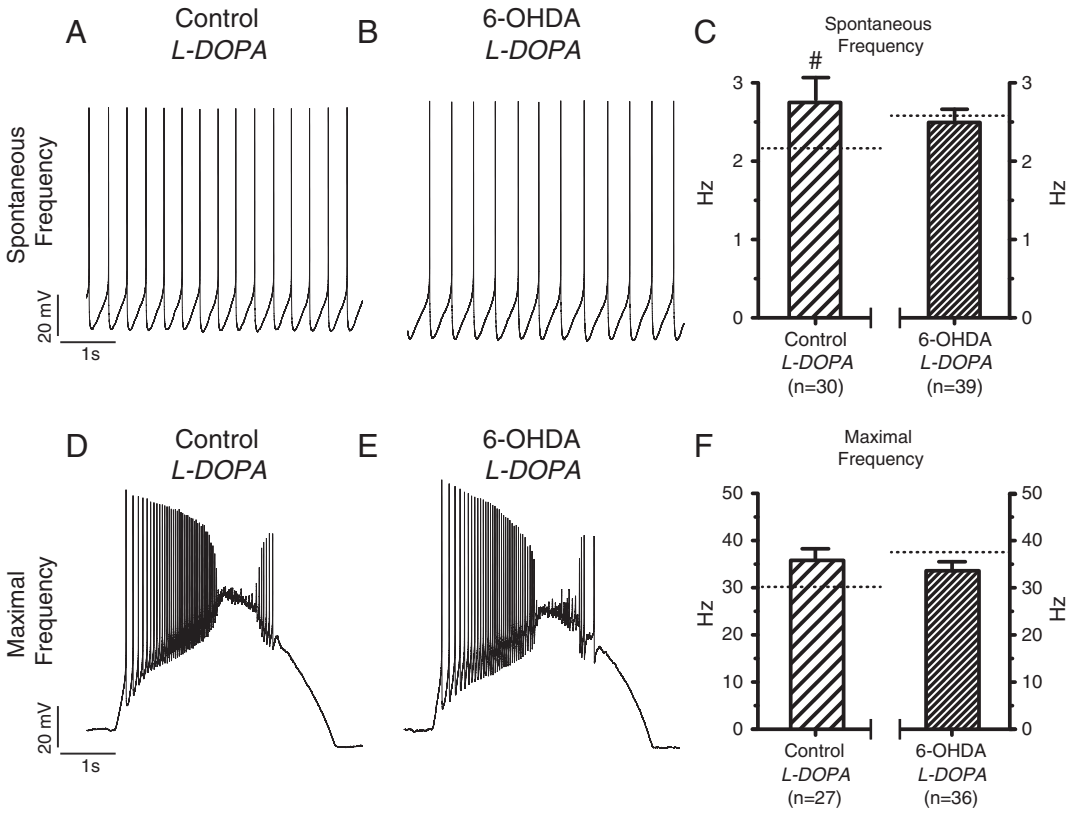

Fig. 4. Electrophysiological changes in serotonin neurons firing discharges after L-DOPA treatment. Following L-DOPA treatment the spontaneous firing was increased in normal/sham-operated ($p = 0.009$; A, C), but unchanged in 6-OHDA animals (B, C), as compared to respective drug-naïve/saline-treated group. The maximal firing discharge showed a strong trend to increase after L-DOPA therapy in normal/sham-operated animals (D, F), while the 6-OHDA showed a trend to decrease (E, F). # = different from drug-naïve/saline-treated animals, here represented by the dashed line in each bar graph.

Discussion

In the current study, we used whole-cell patch-clamp recordings to study the intrinsic electrophysiological properties of immunohistochemically identified serotoninergic DRN neurons in adult mice and compared them with those recorded in mice that had received an intrastriatal injection of 6-OHDA to generate a unilateral Parkinson model. In addition, we explored the effects of L-DOPA treatment on the electrophysiological characteristics in serotoninergic DRN neurons, both in control and 6-OHDA-treated mice. Our data show that severe unilateral DA lesions (i.e. ca.70% striatal DA fiber loss) were sufficient to induce significantly higher spontaneous and maximal in vitro firing rates in serotoninergic DRN neurons compared to those from control mice. These data are in accordance with some but not all in vivo studies, which have shown significant increases in firing frequencies of putative DRN serotonin neurons after 6-OHDA (Chu et al., 2004; Guiard et al., 2008; Wang et al., 2009; Zhang et al., 2007). Interestingly, Wang and colleagues showed a significant increase of 35% in DRN serotonin neurons in vivo in rats from 2.0 Hz in normal controls to 2.7 Hz in 6-OHDA lesioned animals, which can be compared to our in vitro data showing a 18% increase from 2.2 Hz in normal controls to 2.6 Hz in 6-OHDA lesioned mice (Wang et al., 2009). The discrepancy with significantly decreased firing seen by Guiard and colleagues may be explained by the waiting time between the 6-OHDA injection and the recordings. Guiard et al. recorded the cells 10 days following the toxic injection, while in the current study and the in vivo study by Wang and colleagues recorded the cells around 21–28 days and after 3 weeks, respectively (Guiard et al., 2008; Wang et al., 2009).

Our in vitro data set indicates that at least a component of the increased firing of serotonin DRN neurons is mediated by changes in intrinsic excitability. In vivo data have also identified a more bursty firing pattern in serotoninergic DRN neurons after the DA degeneration. As burst firing does only occur in the intact brain, triggered by synaptic inputs, we could not study these types of changes in firing pattern in our in vitro study of synaptically isolated (from non-NMDA glutamate and $GABA_A$, but not $5\text{-}HT_{1A}$ autoreceptor) serotonin DRN neurons. We however identified an increased variability within the interspike interval distribution after 6-OHDA lesion, which was quantified as the coefficient of variation (CV). Increased CV is often related to enhanced burstiness in in vivo recordings, and has indeed been reported by Wang et al. (2009). Although we have not yet identified the biophysical mechanisms responsible for the increased pacemaker frequency in serotonin DRN neurons post 6-OHDA lesions, altered DA neurotransmission on the serotonin system is a likely candidate. First the midbrain receives one of the densest serotonin projections from the DRN in rodents as well as non-human primates (Mackay et al., 1978; Moukhles et al., 1997). Second, direct and dense DA fibers projecting back from the SN and VTA to the DRN has been demonstrated using retrograde tracing techniques (Kalén et al., 1988; Kitahama et al., 2000; Peyron et al., 1995). In addition, studies reported D_2-like receptor expression on the brainstem serotonin neurons, indicating a direct action of DA on the serotonin DRN neurons (Haj-Dahmane, 2001; Mansour et al., 1990). As activation of D_2 receptors on serotonin DRN neurons induces membrane depolarization and increased excitability (Haj-Dahmane, 2001), chronic post-lesion DA depletion might induce a compensatory increase in intrinsic excitability as a form of homeostatic plasticity. It will be interesting to compare D_2-receptor mediated responses in serotonin DRN neurons from control and 6-OHDA lesioned animals. However, the changes in intrinsic excitability might be caused by more indirect changes in the neuronal network, induced by striatal DA depletion.

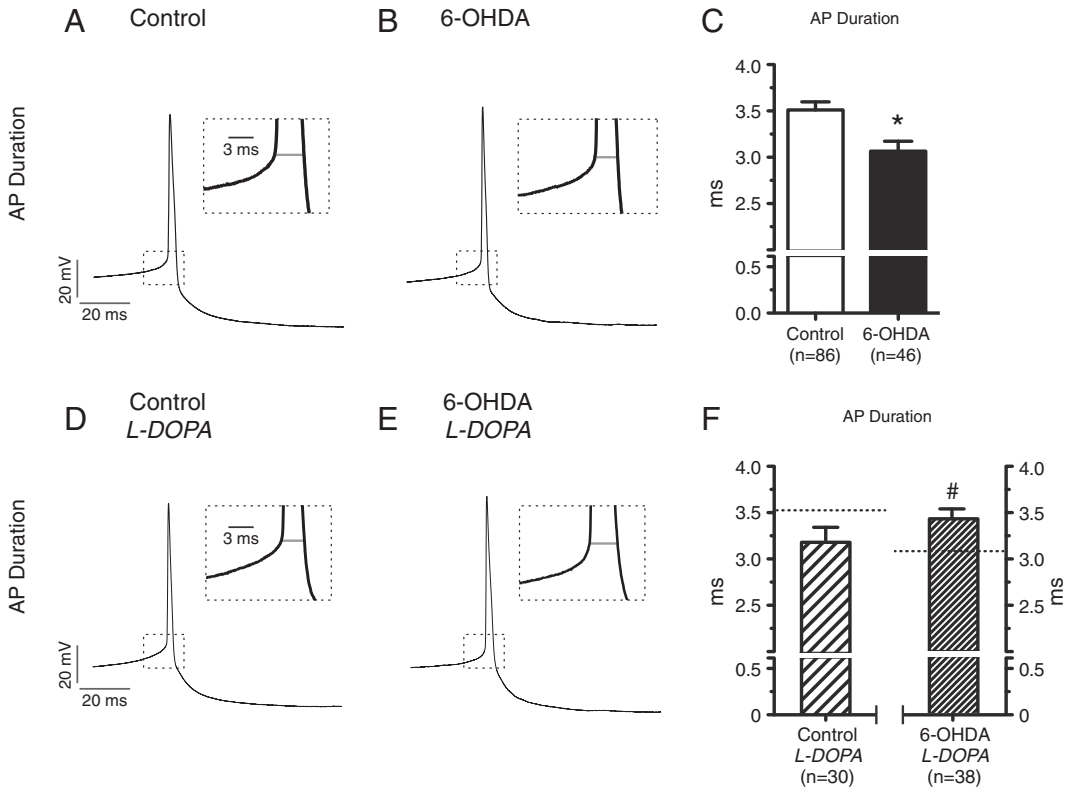

Fig. 5. Changes in action potential (AP) duration in control and 6-OHDA lesioned animals with or without L-DOPA treatment. In accordance with the increase spontaneous firing, the intrastriatal 6-OHDA lesion resulted in a significant decrease of the AP duration ($p = 0.002$; B, C) as compared to normal/sham-operated animals (A, C). Following L-DOPA administration, the AP duration significantly increased in the 6-OHDA group ($p = 0.02$; E, F), as compared to drug naïve/saline-treated animals. This is surprising, while the spontaneous frequency was unaffected by the L-DOPA therapy. The control animals showed a trend to decreased in AP duration after L-DOPA therapy (D, F), but it did not reach significance ($p = 0.05$). The AP duration was designated at the point where the upstroke velocity was 5 mV/ms. * = different from Control; # = different from drug-naive/saline-treated animals, in Panel F represented by the dashed line in each bar graph.

The noradrenaline (NA) network may be one system that could influence the firing properties of the serotonin neurons. It has been demonstrated that the adrenergic agonist phenylephrine can elicit the clocklike firing pattern in serotonin neurons in the DRN (Vandermaelen and Aghajanian, 1983; Kirby et al., 2003). Moreover, 6-OHDA lesions have been shown to affect the NA system (Uretsky & Iversen, 1969). In our study, substantial damage of NA fibers or cells is unlikely, as we used the reuptake inhibitor desipramine. Nevertheless, significant increases in NA concentration have been detected in the striatum, but not in the prefrontal cortex, at 3 to 7 weeks post bilateral intrastriatal, and unilateral medial forebrain bundle (MFB) 6-OHDA lesions (Eskow Jaunarajs et al., 2010; Tadaiesky et al., 2008). In addition, 6-OHDA injections in neonatal rats led to an increase in NA in the raphe nucleus in adulthood (3-months old rats; Molina-Holgado et al., 1993). The studies indicate that enhanced NA signaling might be also present in our model following 6-OHDA lesions and – if so – might influence serotonin DRN firing. However, the noradrenergic system is completely disconnected from the raphe in the coronal in vitro slices used in our study, and thus can be effectively ruled out for causing the observed increases in firing of serotonin DRN neurons post lesion.

It is also possible that the serotonin system was affected in the 6-OHDA model, and it is important to stress that the serotonin system is also significantly affected in PD, with loss of serotonin neurons in the DRN and fibers in the caudate-putamen as well as neurotransmitter (Kish et al., 2008; Kovac et al., 2003). A significant reduction in 5-HT_{1A} receptor binding sites has also been reported in MPTP-intoxicated monkeys, and PD patients (Doder et al., 2003; Frechilla et al., 2001). In addition to the soma and pre-synaptic localized 5-HT_{1A} autoreceptors, a decrease in the postsynaptic 5-HT_{1A} receptors, with high abundance in prefrontal cortex, which through a longer negative feedback loop leading to increased activity in the DRN neurons, may contribute to altered excitability of serotonin DRN neurons reported in this study. Again, a direct assessment of 5-HT_{1A} autoreceptor signaling in serotonin DRN neurons from control and 6-OHDA lesioned mice would be useful in follow-up studies.

Interestingly, serotonin neurons in medial and DRN have been demonstrated to have differences in some electrophysiological properties (Beck et al., 2004; Calizo et. al., 2011). This has also been observed among different serotonin neuron subfields in the DRN (Calizo et al., 2011). Calizo and colleagues showed differences in properties like Resting membrane potential, AHP and responses to a 5-HT receptor agonist (5-CT) in particular between the lateral wings and more dorsomedial subfields of the DRN (Calizo et al., 2011). It is likely however that the location of the cells plays a minor role in our data set, as our recorded cells were placed in the dorsomedial DRN, and not in the lateral wings (see Figs. 2F–H). Moreover, in previous studies, large proportion of the recorded DRN cells was serotonin-negative, as well as not-spontaneous active (Calizo et al., 2011; Kirby et al., 2003). We did not observe too many serotonin-negative cells (>88% of serotonin-positive neurons) in our study, which may be due to our selection of recordings from only spontaneous firing cells. We used spontaneous firing cells as inclusion criteria, as the hallmark in vivo characteristics of serotonin neurons are the 1–5 Hz regular pacemaker activity (Aghajanian and Vandermaelen, 1982). Under in vitro recording conditions both spontaneously active and electrically silent serotonin DRN neurons are encountered (Becks et al., 2004; Brambilla et al., 2007; Jolas et al., 2000; Kirby et al., 2003; Pan et al., 1990), and a selective focus on only active cells might bias the results (Kirby et al., 2003). However, under our recording conditions including the inhibition of $GABA_A$ receptors, almost all identified

serotonin DRN neurons were spontaneously active. This functional homogeneity of synaptically isolated serotonin DRN neurons helped to reveal the changes in intrinsic excitability observed in this population after 6-OHDA lesions.

Another main finding of our study was that chronic L-DOPA treatment subsequent to the 6-OHDA lesion did not reverse the hyperexcitable phenotype of serotonin DRN neurons. This persistent hyperexcitability of serotonin DRN neurons might be a novel mechanism that contributes to the important role of the serotonin system in L-DOPA-induced dyskinesia. Both an increase in serotonin neuron firing discharge following DA depletion alone, and L-DOPA not reversing this phenomenon, may have an important impact on this treatment-induced side effect. It is known that DA, derived from peripherally administered L-DOPA is, activity-dependently, released from serotonin neurons in multiple brain regions, including the nigrostriatal pathway (Navailles et al., 2010a). This strengthens the facts that the serotonin system is the major player in the development and maintenance of L-DOPA-induced dyskinesias in rodents and non-human primates (Bezard et al., 2013; Carta et al., 2007; Munoz et al., 2008; Rylander et al., 2010). It is suggested that the intermittent and pulsatile release of DA, causing high peaks of extracellular DA, is associated with the development and expression of the dyskinesias (de la Fuente-Fernandez et al., 2004; Olanow et al., 2006). Therefore, it is feasible to believe that an increased firing of the DRN serotonin neurons, following DA denervation of the nigrostriatal pathway, will lead to a more rapid release of converted DA (as compared to DA release in normal firing cells), and in turn aggravated peaks of extracellular DA. At these significant DA peaks, the expression of L-DOPA-induced dyskinesia is likely to also be more severe. These more rapid peaks possibly are resulting in further abnormal swings in extracellular DA content. In addition, as L-DOPA treatment cannot reverse the firing rate of these neurons, the swing will remain supernormal and increase the risk of developing dyskinesia. This is likely to be further aggravated by the indications that the serotonin release from terminals is decreased after acute L-DOPA administration (Navailles et al., 2010b), which in turn decreased serotonin$_{1A}$ autoreceptor stimulation, and that the serotonin neurons lack an autoregulatory feedback via D_2 receptors (that are found on the DA terminals in the striatum) to control this DA release.

Similar to Lundblad et al. (2004), using the same intrastriatal lesion model resulting in about 70% DA fiber denervation in the striatum, and L-DOPA dose of 6 mg/kg, we indeed observed occasional expression of L-DOPA-induced dyskinesia in the few animals that we tested for abnormal involuntary movement (AIMs) with low frequency (average sum of limb, orolingual, and axial dyskinesias — scored every 20 min — 6.3 ± 2.3 AIM scores; n = 4). In our study, however, with the limited number of mice and the low frequencies of dyskinesias, it was not suitable to correlate these AIMs with the respective electrophysiological properties. It would nevertheless be of great interest, in a follow-up study, to correlate in particular the firing properties of the serotonin neurons with the animals' individual expression patterns and frequency of L-DOPA-induced dyskinesias. To achieve this, higher doses of L-DOPA in the partial 6-OHDA lesion model should be used here to induce more severe AIMs, or to use the 6-OHDA MFB model of PD, which shows more complete nigrostriatal DA denervation, and subsequently more severe dyskinesias following chronic L-DOPA treatment (Lundblad et al., 2004). When using the MFB lesion model in mice however one needs to consider the very high mortality rates following the 6-OHDA injection (Lundblad et al., 2004). In addition, significant lesions of the VTA, which are also caused in the MFB model, might have distinct effects on the serotonin DRN neuronal physiology (for review see Di Giovanni et al., 2008).

In addition, L-DOPA treatment appears to induce its own type of plastic changes of intrinsic electrophysiological properties in serotonin DRN neurons as evident from the higher pacemaker frequencies in neurons recorded from non-lesioned, but L-DOPA treated mice. Here, it is further unlikely that NA plays the major role in the increase in spontaneous firing, as L-DOPA treatment has shown not to affect the NA levels in normal animals, and even normalizes the increase seen after 6-OHDA lesions (Eskow Jaunarajs et al., 2010). Again, the underlying biophysical mechanism of this L-DOPA induced plasticity in serotonin DRN neurons needs to be identified in future studies.

In conclusion, our study identified novel plastic changes in intrinsic excitability of identified serotonin DRN neurons in response to both striatal DA depletion and L-DOPA treatment. These changes in excitability might contribute both to the PD and L-DOPA-induced dyskinesias as discussed above. The important next step would be the identification of altered receptor and ion channel mechanisms that cause the reported changes in excitability of serotonin DRN neurons, first identified in this study.

Acknowledgment

We would like to thank Beatrice Kern, Annika Parg, and Alois Kreuzer for their technical support of this experiment. The project based on this report was funded by the program for medical genome research with financial support from the Federal Ministry of Education and Research (BMBF) under the support code 01GS08141 (Liss/Roeper). The authors are responsible for the content of this publication. TC was supported by the NGFN-plus Programm, NeuroNetz, TP-13: "Dopaminergic dysfunction and molecular pathways to selective neurodegeneration: from mouse models to Parkinson disease" to Prof. Jochen Roeper (Goethe University Frankfurt, Germany), and Prof. Birgit Liss (University of Ulm, Germany). B.L. was funded by the Alfried Krupp award. All authors declare no conflict of interest.

References

Aghajanian, G.K., Vandermaelen, C.P., 1982. Intracellular identification of central noradrenergic and serotonergic neurons by a new double labeling procedure. J. Neurosci. 2 (12), 1786–1792.
Alvarez-Fischer, D., Henze, C., Strenzke, C., Westrich, J., Ferger, B., Höglinger, G.U., Oertel, W.H., Hartmann, A., 2008. Characterization of the striatal 6-OHDA model of Parkinson's disease in wild type and alpha-synuclein-deleted mice. Exp. Neurol. 210 (1), 182–193.
Arai, R., Karasawa, N., Geffard, M., Nagatsu, T., Nagatsu, I., 1994. Immunohistochemical evidence that central serotonin neurons produce dopamine from exogenous L-DOPA in the rat, with reference to the involvement of aromatic L-amino acid decarboxylase. Brain Res. 667 (2), 295–299.
Arai, R., Karasawa, N., Geffard, M., Nagatsu, I., 1995. L-DOPA is converted to dopamine in serotonergic fibers of the striatum of the rat: a double-labeling immunofluorescence study. Neurosci. Lett. 195 (3), 195–198.
Arai, R., Karasawa, N., Nagatsu, I., 1996. Aromatic L-amino acid decarboxylase is present in serotonergic fibers of the striatum of the rat A double-labeling immunofluorescence study. Brain Res. 706 (1), 177–179.
Beck, S.G., Pan, Y.Z., Akanwa, A.C., Kirby, L.G., 2004. Median and dorsal raphe neurons are not electrophysiologically identical. J. Neurophysiol. 91 (2), 994–1005.
Bezard, E., Tronci, E., Pioli, E.Y., Li, Q., Porras, G., Björklund, A., Carta, M., 2013. Study of the antidyskinetic effect of eltoprazine in animal models of levodopa-induced dyskinesia. Mov. Disord. 2013. http://dx.doi.org/10.1002/mds.25366.
Bonifati, V., Fabrizio, E., Cipriani, R., Vanacore, N., Meco, G., 1994. Buspirone in levodopa-induced dyskinesias. Clin. Neuropharmacol. 17 (1), 73–82 (Feb).
Brambilla, D., Franciosi, S., Opp, M.R., Imeri, L., 2007. Interleukin-1 inhibits firing of serotonergic neurons in the dorsal raphe nucleus and enhances GABAergic inhibitory post-synaptic potentials. Eur. J. Neurosci. 26 (7), 1862–1869.
Calizo, L.H., Akanwa, A., Ma, X., Pan, Y.Z., Lemos, J.C., Craige, C., Heemstra, L.A., Beck, S.G., 2011. Raphe serotonin neurons are not homogenous: electrophysiological, morphological and neurochemical evidence. Neuropharmacology 61 (3), 524–543.
Carlsson, T., Carta, M., Winkler, C., Björklund, A., Kirik, D., 2007. Serotonin neuron transplants exacerbate L-DOPA-induced dyskinesias in a rat model of Parkinson's disease. J. Neurosci. 27 (30), 8011–8022.
Carta, M., Carlsson, T., Kirik, D., Björklund, A., 2007. Dopamine released from 5-HT terminals is the cause of L-DOPA-induced dyskinesia in Parkinsonian rats. Brain 130 (Pt 7), 1819–1833.
Chu, Y.X., Liu, J., Feng, J., Wang, Y., Zhang, Q.J., Li, Q., 2004. Changes of discharge rate and pattern of 5-hydroxytrypamine neurons of dorsal raphe nucleus in a rat model of Parkinson's disease. Sheng Li Xue Bao 56 (5), 597–602.
de la Fuente-Fernández, R., Sossi, V., Huang, Z., Furtado, S., Lu, J.Q., Calne, D.B., Ruth, T.J., Stoessl, A.J., 2004. Levodopa-induced changes in synaptic dopamine levels increase with progression of Parkinson's disease: implications for dyskinesias. Brain 127 (Pt 12), 2747–2754.
Di Giovanni, G., Di Matteo, V., Pierucci, M., Esposito, E., 2008. Serotonin-dopamine interaction: electrophysiological evidence. Prog. Brain Res. 172, 45–71.

Doder, M., Rabiner, E.A., Turjanski, N., Lees, A.J., Brooks, D.J., 2003. Tremor in Parkinson's disease and serotonergic dysfunction: an 11C-WAY 100635 PET study. Neurology 60 (4), 601–605.
Eskow Jaunarajs, K.L., Dupre, K.B., Ostock, C.Y., Button, T., Deak, T., Bishop, C., 2010. Behavioral and neurochemical effects of chronic L-DOPA treatment on nonmotor sequelae in the hemiparkinsonian rat. Behav. Pharmacol. 21 (7), 627–637.
Frechilla, D., Cobreros, A., Saldise, L., Moratalla, R., Insausti, R., Luquin, M., Del Río, J., 2001. Serotonin 5-HT(1A) receptor expression is selectively enhanced in the striosomal compartment of chronic parkinsonian monkeys. Synapse 39 (4), 288–296.
Guiard, B.P., El Mansari, M., Merali, Z., Blier, P., 2008. Functional interactions between dopamine, serotonin and norepinephrine neurons: an in-vivo electrophysiological study in rats with monoaminergic lesions. Int. J. Neuropsychopharmacol. 11 (5), 625–639.
Haj-Dahmane, S., 2001. D2-like dopamine receptor activation excites rat dorsal raphe 5-HT neurons in vitro. Eur. J. Neurosci. 14 (1), 125–134.
Hollister, A.S., Breese, G.R., Mueller, R.A., 1979. Role of monoamine neural systems in L-dihydroxyphenylalanine-stimulated activity. J. Pharmacol. Exp. Ther. 208 (1), 37–43.
Jolas, T., Aghajanian, G.K., 1997. Opioids suppress spontaneous and NMDA-induced inhibitory postsynaptic currents in the dorsal raphe nucleus of the rat in vitro. Brain Res. 755 (2), 229–245.
Jolas, T., Nestler, E.J., Aghajanian, G.K., 2000. Chronic morphine increases GABA tone on serotonergic neurons of the dorsal raphe nucleus: association with an up-regulation of the cyclic AMP pathway. Neuroscience 95 (2), 433–443.
Kalén, P., Skagerberg, G., Lindvall, O., 1988. Projections from the ventral tegmental area and mesencephalic raphe to the dorsal raphe nucleus in the rat. Evidence for a minor dopaminergic component. Exp. Brain Res. 73 (1), 69–77.
Kirby, L.G., Pernar, L., Valentino, R.J., Beck, S.G., 2003. Distinguishing characteristics of serotonin and non-serotonin-containing cells in the dorsal raphe nucleus: electrophysiological and immunohistochemical studies. Neuroscience 116 (3), 669–683.
Kirik, D., Georgievska, B., Burger, C., Winkler, C., Muzyczka, N., Mandel, R.J., Bjorklund, A., 2002. Reversal of motor impairments in parkinsonian rats by continuous intrastriatal delivery of L-dopa using rAAV-mediated gene transfer. Proc. Natl. Acad. Sci. U.S.A. 2;99 (7), 4708–4713.
Kish, S.J., Tong, J., Hornykiewicz, O., Rajput, A., Chang, L.J., Guttman, M., Furukawa, Y., 2008. Preferential loss of serotonin markers in caudate versus putamen in Parkinson's disease. Brain 131, 120–131.
Kitahama, K., Nagatsu, I., Geffard, M., Maeda, T., 2000. Distribution of dopamine-immunoreactive fibers in the rat brainstem. J. Chem. Neuroanat. 18 (1–2), 1–9.
Kovacs, G.G., Klöppel, S., Fischer, I., Dorner, S., Lindeck-Pozza, E., Birner, P., 2003. Nucleus-specific alteration of raphe neurons in human neurodegenerative disorders. Neuroreport 14 (1), 73–76.
Lammel, S., Hetzel, A., Häckel, O., Jones, I., Liss, B., Roeper, J., 2008. Unique properties of mesoprefrontal neurons within a dual mesocorticolimbic dopamine system. Neuron 57 (5), 760–773.
Lundblad, M., Picconi, B., Lindgren, H., Cenci, M.A., 2004. A model of L-DOPA-induced dyskinesia in 6-hydroxydopamine lesioned mice: relation to motor and cellular parameters of nigrostriatal function. Neurobiol. Dis. 16 (1), 110–123.
Mackay, A.V., Yates, C.M., Wright, A., Hamilton, P., Davies, P., 1978. Regional distribution of monoamines and their metabolites in the human brain. J. Neurochem. 30 (4), 841–848.
Mansour, A., Meador-Woodruff, J.H., Bunzow, J.R., Civelli, O., Akil, H., Watson, S.J., 1990. Localization of dopamine D2 receptor mRNA and D1 and D2 receptor binding in the rat brain and pituitary: an in situ hybridization-receptor autoradiographic analysis. J. Neurosci. 10 (8), 2587–2600.
Molina-Holgado, E., Dewar, K.M., Grondin, L., van Gelder, N.M., Reader, T.A., 1993. Changes of amino acid and monoamine levels after neonatal 6-hydroxydopamine denervation in rat basal ganglia, substantia nigra, and Raphe nuclei. J. Neurosci. Res. 1;35 (4), 409–418.
Moukhles, H., Bosler, O., Bolam, J.P., Vallée, A., Umbriaco, D., Geffard, M., Doucet, G., 1997. Quantitative and morphometric data indicate precise cellular interactions between serotonin terminals and postsynaptic targets in rat substantia nigra. Neuroscience 76 (4), 1159–1171.
Muñoz, A., Li, Q., Gardoni, F., Marcello, E., Qin, C., Carlsson, T., Kirik, D., Di Luca, M., Björklund, A., Bezard, E., Carta, M., 2008. Combined 5-HT1A and 5-HT1B receptor agonists for the treatment of L-DOPA-induced dyskinesia. Brain 131 (Pt 12), 3380–3394.
Navailles, S., Bioulac, B., Gross, C., De Deurwaerdère, P., 2010a. Serotonergic neurons mediate ectopic release of dopamine induced by L-DOPA in a rat model of Parkinson's disease. Neurobiol. Dis. 38 (1), 136–143.
Navailles, S., Benazzouz, A., Bioulac, B., Gross, C., De Deurwaerdère, P., 2010b. High-frequency stimulation of the subthalamic nucleus and L-3,4-dihydroxyphenylalanine inhibit in vivo serotonin release in the prefrontal cortex and hippocampus in a rat model of Parkinson's disease. J. Neurosci. 10;30 (6), 2356–2364.
Ng, K.Y., Chase, T.N., Colburn, R.W., Kopin, I.J., 1970. L-Dopa-induced release of cerebral monoamines. Science 170 (953), 76–77.
Ng, K.Y., Colburn, R.W., Kopin, I.J., 1971. Effects of L-dopa on efflux of cerebral monoamines from synaptosomes. Nature 230 (5292), 331–332.
Olanow, C.W., Obeso, J.A., Stocchi, F., 2006. Continuous dopamine-receptor treatment of Parkinson's disease: scientific rationale and clinical implications. Lancet Neurol. 5 (8), 677–687.
Pan, Z.Z., Williams, J.T., Osborne, P.B., 1990. Opioid actions on single nucleus raphe magnus neurons from rat and guinea-pig in vitro. J. Physiol. 427, 519–532.
Peyron, C., Luppi, P.H., Kitahama, K., Fort, P., Hermann, D.M., Jouvet, M., 1995. Origin of the dopaminergic innervation of the rat dorsal raphe nucleus. Neuroreport 116 (18), 2527–2531.
Rylander, D., Parent, M., O'Sullivan, S.S., Dovero, S., Lees, A.J., Bezard, E., Descarries, L., Cenci, M.A., 2010. Maladaptive plasticity of serotonin axon terminals in levodopa-induced dyskinesia. Ann. Neurol. 68 (5), 619–628.
Tadaiesky, M.T., Dombrowski, P.A., Figueiredo, C.P., Cargnin-Ferreira, E., Da Cunha, C., Takahashi, R.N., 2008. Emotional, cognitive and neurochemical alterations in a premotor stage model of Parkinson's disease. Neuroscience 156 (4), 830–840.
Uretsky, N.J., Iversen, L.L., 1969. Effects of 6-hydroxydopamine on noradrenaline-containing neurones in the rat brain. Nature 221 (5180), 557–559 (Feb 8).
Vandermaelen, C.P., Aghajanian, G.K., 1983. Electrophysiological and pharmacological characterization of serotonergic dorsal raphe neurons recorded extracellularly and intracellularly in rat brain slices. Brain Res. 19;289 (1-2), 109–119.
Wang, S., Zhang, Q.J., Liu, J., Wu, Z.H., Wang, T., Gui, Z.H., Chen, L., Wang, Y., 2009. Unilateral lesion of the nigrostriatal pathway induces an increase of neuronal firing of the midbrain raphe nuclei 5-HT neurons and a decrease of their response to 5-HT(1A) receptor stimulation in the rat. Neuroscience 159 (2), 850–861.
Zhang, Q.J., Gao, R., Liu, J., Liu, Y.P., Wang, S., 2007. Changes in the firing activity of serotonergic neurons in the dorsal raphe nucleus in a rat model of Parkinsons disease. Sheng Li Xue Bao 59 (2), 183–189.